Role of the *Dictyostelium* 30 kDa Protein in Actin Bundle Formation[†]

Ruth Furukawa* and Marcus Fechheimer

Department of Cellular Biology, University of Georgia, Athens, Georgia 30602

Received January 25, 1996; Revised Manuscript Received April 3, 1996[⊗]

ABSTRACT: We have studied the formation of bundles in mixtures of actin with the *Dictyostelium* 30 kDa actin-bundling protein as a function of 30 kDa protein concentration, actin concentration, and filament length. The presence of the 30 kDa protein promotes formation of filament bundles at actin concentrations and filament lengths that are not spontaneously aligned into liquid crystalline domains in the absence of the 30 kDa protein. Bundle formation in the presence of the 30 kDa protein was observed over a broad range of actin filament lengths and concentrations. Bundling was filament length dependent, and short filaments were more efficiently bundled. Bundles formed at actin concentrations as low as 2 μM. The volume fraction of the bundled portion and concentrations of actin and the 30 kDa protein in the bundled portion were measured using a sedimentation assay. Bundles have concentrations of actin and 30 kDa protein that are 10−20 and 5−20 times, respectively, greater than that of the bulk solution. Computer modeling reveals that bundling of actin by a bundling protein increases both the mean length and the polydispersity of the length distribution, factors which lower the actin concentration required for spontaneous alignment within the bundle. We propose that entropy-driven spontaneous ordering may contribute to bundle formation in two ways. Bundling of actin creates longer aggregates with a more polydisperse length distribution in which actin aligns spontaneously within the bundle at very low concentrations. In addition, bundling creates locally high concentrations of actin within these aggregates that will spontaneously align, providing an additional driving force for bundle ordering.

Cytoplasm is a complex substance which can be described as viscoelastic, inhomogeneous, anisotropic, thixotropic, and dynamic. Interconversion of cytoplasm between highly structured gel and more fluid sol states is associated with changes in cell shape and movement (Frey-Wyssling, 1953; Seifritz, 1942). Detailed studies of the physical and structural properties of cytoplasm (Elson, 1988; Luby-Phelps et al., 1988; Taylor & Condeelis, 1979) provide a foundation for molecular theories and hypotheses regarding the contributions of gel to sol transitions to cellular movements (Condeelis, 1993; Janson et al., 1991; Kolega et al., 1991; Taylor & Fechheimer, 1982). Since cross-linked actin structures are proposed to make a major contribution to the physical and structural properties of cytoplasm, molecular understanding of the dynamic changes in cytoplasmic structure accompanying cell movements has been sought through studies of reconstituted models and mixtures of purified proteins.

Cross-linked actin structures both in cytoplasm and in vitro can form either a random, isotropic network (gel) or an ordered, anisotropic array (bundle). A number of factors have been proposed to regulate the geometry of the type of structure formed, including the presence of shear forces (Cortese & Frieden, 1988, 1990) and the type of actin cross-linking protein (Matsudaira, 1991; Otto, 1994). Differences in the activity of isotypes of α-actinin have been attributed to differences in the affinity for actin (Wachsstock et al., 1993, 1994) and molecular length (Meyer & Aebi, 1990) of α-actinin. The length of the actin filaments is another important factor. Longer actin filaments are more readily gelled (Nunnally et al., 1980; Yin et al., 1980) and immobilized by filamin (Cortese & Frieden, 1990), whereas a reduction of actin filament length was reported to promote bundling of actin filaments by α-actinin (Maciver et al., 1991). Finally, the spontaneous alignment of actin filaments accompanying the phase transition from the isotropic to liquid crystalline state is a potential driving force for the formation of oriented actin filament networks (Furukawa et al., 1993; Coppin & Leavis, 1992; Suzuki et al., 1991; Kerst et al., 1990; Buxbaum et al., 1987).

The *Dictyostelium* 30 000 dalton protein (30 kDa protein) is a calcium-sensitive actin binding protein which can cross-link actin filaments (Furukawa & Fechheimer, 1990; Fechheimer, 1987; Fechheimer & Taylor, 1984) into bundles. The 30 kDa protein is localized in the filopodia, cortical cytoskeleton (Johns et al., 1988; Fechheimer, 1987), phagocytic cup, cleavage furrow (Furukawa & Fechheimer, 1994), and sites of cell to cell contact (Fechheimer et al., 1994). A proteolytic fragment of the 30 kDa protein has been shown to cross-link actin filaments into isotropic arrays but lacks bundling activity (Fechheimer & Furukawa, 1993). In the present study, we have employed transmission of polarized light, polarization microscopy, polarized light scattering (Fechheimer & Furukawa, 1993; Furukawa et al., 1993), and a sedimentation approach to investigate the effects of filament length, actin concentration, and bundling protein concentration on the formation of bundled aggregates of F-actin. The results of our studies and computer simulations support a novel model of the bundling process in mixtures of actin with the *Dictyostelium* 30 kDa protein. A preliminary account of this work was presented at the annual meeting of the American Society of Cell Biology in New Orleans, LA, in December 1993 (Furukawa & Fechheimer, 1993).

[†] Supported by NSF MCB-9405738 to M.F.

* Author to whom correspondence should be addressed. Telephone: 706-542-3338. Fax: 706-542-4271. E-mail: furukawa@cb.uga.edu.

[⊗] Abstract published in *Advance ACS Abstracts,* May 15, 1996.

S0006-2960(96)00192-4 CCC: $12.00

MATERIALS AND METHODS

Purification of Rabbit Skeletal Muscle Actin. Actin was purified from an acetone powder of rabbit skeletal muscle essentially as described by Spudich and Watt (1971) with two cycles of assembly and sedimentation through 0.6 M KCl and then fractionated on a 2.5 × 64 cm column of Sephadex G-150 in 2 mM Tris, 0.2 mM ATP, 0.2 mM $CaCl_2$, 0.2 mM dithiothreitol, and 0.02% sodium azide (pH 8.0) (MacLean-Fletcher & Pollard, 1980). Actin was held in dialysis for at most 7 days with buffer changes every 24 h. The concentration range of actin studied is limited to the concentration directly eluted from the G-150 column. Further concentration of actin was not performed to minimize endogenous sources of nucleation other than that induced by gelsolin and to ensure that all actin present was capable of polymerization. The concentration of G-actin was determined using an extinction coefficient of 0.62 mg^{-1} mL cm^{-1} at 290 nm.

Purification of the 30 kDa Actin Bundling Protein. The *Dictyostelium* 30 kDa protein was purified as previously described (Fechheimer & Furukawa, 1991). The concentration was measured using the bicinchoninic acid method (Smith et al., 1985) using bovine serum albumin as the standard. For some experiments, recombinant *Dictyostelium* 30 kDa protein was purified from *Escherichia coli* (R. W. L. Lim and M. Fechheimer, unpublished).

Purification of Gelsolin. Gelsolin was purified by the method of Cooper et al. (1987) as described previously (Furukawa et al., 1993). Gelsolin concentration was measured using the bicinchoninic acid method (Smith et al., 1985) using bovine serum albumin as the standard. The functional activity of the gelsolin was assayed by enhancement of the fluorescence of NBD−actin upon gelsolin binding (Coué & Korn, 1985). NBD−actin was prepared as described previously (Detmers et al., 1981).

Light Scattering. Light scattering was performed as previously described (Fechheimer & Furukawa, 1993). Briefly, mixtures of gelsolin, freshly gel-filtered actin, and the 30 kDa protein were polymerized in 0.5 cm fluorescence cuvettes with 20 mM Pipes, 1 mM ATP, 50 μM $MgCl_2$, 50 mM KCl, 5 mM EGTA, 0.2 mM dithiothreitol, and 0.02% sodium azide (pH 7.0). The cuvettes, pipette tips, and glassware were rinsed exhaustively with water previously filtered through a 0.22 μm filter in a laminar flow hood to remove dust. All buffers and proteins were filtered through a 0.22 μm filter into dust free glassware. The protein solutions were mixed in the cuvettes and degassed, salts needed to induce assembly of the actin were added, and then the solutions were gently mixed with six strokes using a plastic paddle. The cuvettes were then capped and held at room temperature for 24 h before the measurements.

Light scattering measurements were performed at a scattering angle of 90° in a Perkin-Elmer LS-5 spectrofluorometer with polarizing optics. Conventional terminology is that the first letter (uppercase, H or V) indicates the vertical or horizontal plane of polarization of the scattered light, and the second letter (lower case, h or v) indicates the plane of polarization of the incident light. The Vv and Hv components of the scattered light were measured. Measurements from three to six independent samples were recorded. The mean value and standard deviations were calculated.

Light scattering can detect the size and shape of structures in solution but cannot discern the differences between actin bundles and actin nematic liquid crystalline phase. However, this technique is very sensitive to microscopic changes below the resolution of a microscope and has the additional advantage of providing quantitative data.

Transmission of Light through Crossed Polarizers. Transmission of polarized light was observed through each sample in which light scattering was measured with dichroic sheet polarizers (catalog no. 47 36 00; Carl Zeiss, Inc., Thornwood, NY) as described previously (Furukawa et al., 1993).

This assay detects the difference between isotropic and ordered structures in solution by the appearance of birefringence. It does not allow distinction between the presence of actin bundles from the nematic liquid crystalline phase of actin since both of these structures are birefringent.

Polarization Microscopy. Actin, gelsolin, and the 30 kDa protein were mixed in varying concentrations using solution conditions described above for light scattering. Samples for polarization microscopy were mounted using clear nail polish to seal the cover slips to prevent evaporation and drying. A rectified polarization objective (40×, N. A. 0.65, Nikon Inc., Garden City, NY), a $^1/_4\,\lambda$ wave plate, and a 16 mm condenser (N. A. 0.52) were employed on a Zeiss Ultraphot II using a 200 W mercury arc illuminator. Images were recorded on Tri-X film.

Polarized light microscopy also detects the difference between isotropic and ordered structures in solution by the appearance of birefringence. It also allows nematic liquid crystalline domains to be distinguished from actin bundles by their characteristic visual appearances. The limitation of polarized microscopy is inherent in the spatial resolution of microscopy. Thus, very small quantities or small structures will not be detected.

Determination of Volume Fractions in the Isotropic and Bundled Portions. Mixtures of gelsolin, the 30 kDa protein, and actin prepared as described for light scattering studies were allowed to assemble in 100 μL capillary pipettes for 24 h. The capillaries were centrifuged at 13 000*g* for 25 min in a hematocrit (Clay Adams, Franklin Lakes, NJ). These conditions were empirically determined to be sufficient to maximally sediment the actin bundles at low *g* forces. Specifically, increases in time of sedimentation at 13 000*g* did not result in tighter packing of the pellet and/or a decrease in the volume fraction of the bundled portion. Dark field microscopy was performed on each sample. Measurements were obtained visually using a Zeiss IM 35 microscope equipped with a 4× objective either by use of an eyepiece recticle or with magnification using an ISIT camera (DAGE-MTI, model 66x, Michigan City, IN). The magnification of the camera and monitor were calibrated using a stage micrometer. A typical sample is shown in Figure 1. The height of the bundled portion, the total sample, and the diameter of the capillary were recorded. The capillary pipettes were subsequently cracked, and the supernatants were sampled. The polypeptides were resolved on 12% acrylamide gels using SDS−PAGE and stained with Coomassie blue. The amount of protein was determined by densitometry (Molecular Dynamics, Sunnyvale, CA) using purified actin to obtain a standard calibration curve. Measurements from three to six independent samples were recorded. The mean value and standard deviations were calculated.

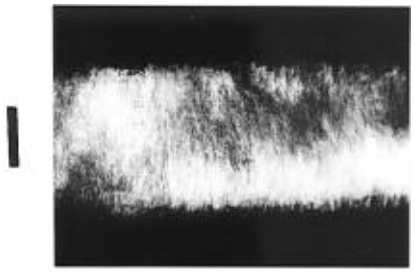

FIGURE 1: Dark field microscopy of a capillary after sedimentation showing the fibrillar texture of the actin and 30 kDa protein bundles. Bar = 1 mm.

The volumes of the sample and bundled portions were calculated using the measured heights and diameter of the sample. The concentration of the actin and 30 kDa protein in the supernatant and bundled portions was calculated from the amount of protein determined by SDS−PAGE and the volume of each portion. The volume fraction of the bundled portion was calculated by dividing the volume of the bundled portion by the total volume of the solution. Measurements from three to six independent samples were recorded. The mean value and standard deviations were calculated.

The advantage of sedimentation is that small quantities of bundled actin can be quantified after physical separation of the bundles from the remainder of the solution. The concentrations of both the actin and the 30 kDa protein in the bundles and supernatant can be determined due to the physical separation that sedimentation provides. This information cannot be determined by the above techniques. Furthermore, the volume fraction of the bundled and supernatant portions can be determined. This is a key quantity in theoretical predictions of isotropic to nematic phase transitions. However, there are limitations on the centrifugal force that may be applied to a glass capillary. Thus, the protein concentrations are minimal estimates since greater compaction and sedimentation may occur at higher centrifugal forces.

Computational Modeling of Actin Bundling. The change in the actin filament length distribution created by the bundling of filaments by a bundling protein was investigated by computer modeling. Calculations were performed to analyze the effect of varying the ratio of the bundling protein to actin filaments and of actin filament length. Actin bundles were formed by the following algorithm. The Box−Muller algorithm (Honerkamp, 1994) was employed to randomly generate the initial filament length distribution, a constant number of filaments which had a Gaussian length distribution about a given mean length and a standard deviation which was 10% of the mean value. Two filaments were randomly selected from the initial population using the ran1 algorithm (Press et al., 1988). The bundling protein was allowed to bind randomly along either filament with a fixed geometry of 90° with respect to the filament to form a bundled structure. In this manner, all of the actin filaments are constrained to a parallel orientation. A new length was calculated and was introduced into the actin population, while the two filaments which were cross-linked were deleted. This iterative calculation continued until all the bundling protein was bound. These conditions allow actin filaments that are cross-linked to other actin filaments to be further cross-linked but can contain only one cross-link between any two filaments. In this manner, bundles can cross-link to other bundles. The mean length, the standard deviation of the new population, and the mole fraction of total actin that is present in cross-linked structures were calculated. No disassociation/reassociation reactions of the bundling protein were allowed, and the geometry of every molecule of the bundling protein was constrained to form a productive cross-link. Filament numbers were varied from 2500 to 500 in increments of 500. Numbers less than 1000 were insufficient to generate stable solutions to the calculations. Each calculation was repeated ten times with 2000 filaments to ensure that random sampling had occurred.

The limitations which are inherent in this calculation are that the bundling protein is all bound with no association or dissociation reactions allowed and that each molecule of bundling protein is constrained to form a productive cross-link with a fixed geometry which results in bundle formation. Under experimental conditions, binding is governed by affinity with multiple association/dissociation reactions, the geometry of the bundling protein binding to the actin filament is unknown, and diffusion of the proteins occurs so that rearrangement of the actin filaments within a bundle is possible.

RESULTS

The formation of cross-linked structures in mixtures of actin and the 30 kDa protein has been examined using transmission of light through crossed polarizers, polarized light microscopy, polarized light scattering, and low-speed sedimentation as a function of three experimental variables: the concentration of actin which was varied from 2 to 48 μM; the concentration of the 30 kDa protein which was varied from 0.5 to 1 to 2 μM; and the average filament length which was controlled by varying the ratio of actin to gelsolin from 222:1 (0.6 μm) to 555:1 (1.5 μm) to 1111:1 (3.0 μm) to 1778:1 (4.9 μm) at each actin concentration and 30 kDa protein concentration.

Macroscopic and Microscopic Observations of Birefringence. Previous results for solutions of actin alone with filament lengths between 1.5 and 4.9 μm indicated formation of a nematic liquid crystalline phase as detected by transmission of light through crossed polarizers at actin concentrations between 57.6 and 48.7 μM (Furukawa et al., 1993) (for a representative sample, see Figure 2A). No nematic liquid crystalline phase was detected for 0.6 μm filaments at actin concentrations as great as 72 μM.

The presence of as little as 0.5 μM of the 30 kDa protein in solutions containing a minimum of 24 μM actin at all filament lengths studied resulted in a birefringent solution as shown by the characteristic swirled pattern in Figure 2C. Although the 30 kDa protein has been shown to cross-link actin into bundles (Fechheimer, 1987), it was conceivable that the 30 kDa protein promoted actin segregation into nematic liquid crystalline domains and that the solution birefringence resulted from either liquid crystalline domains, actin bundles, or a mixture of both. To investigate this possibility, polarization microscopy was employed to examine the nature of the birefringent structures formed in solutions of actin and the 30 kDa protein. Actin nematic liquid crystalline domains exhibited a maltese cross pattern (Donald & Windle, 1992) as shown in Figure 2B. By contrast, the actin bundles appeared needle-like and randomly oriented in solution as shown in Figure 2D.

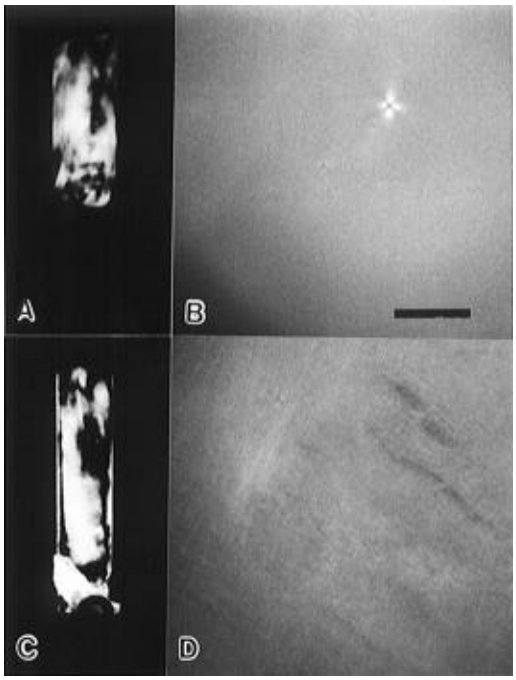

FIGURE 2: Macroscopic and microscopic observation of birefringence. Polarized transmitted light images of a solution of actin (A) or a solution of actin and the 30 kDa protein (C). Polarized light micrograph images of a solution of actin (B) or a solution of actin and the 30 kDa protein (D). The actin:gelsolin ratio was 1778:1 with 57.6 μM actin (A and B). The actin:gelsolin ratio was 222:1 with either 28.8 or 36 μM actin (C and D, respectively) and 2 μM 30 kDa protein. The swirled pattern obtained by macroscopic observations of birefringence can indicate the presence of either nematic liquid crystalline regions or bundles. The distinction between these possibilities is obtained through the microscopic observations of birefringence, nematic liquid crystalline regions (B) and bundles (D). Bar = 15 μm.

Bundle formation was a function of actin filament length and the concentration of both actin and the 30 kDa protein. For 0.6 μm (222:1 actin:gelsolin) filaments in the presence of any quantity of the 30 kDa protein at actin concentrations $\geq$24 μM, only actin bundles were observed. For 4.9 μm (1778:1 actin:gelsolin) filaments in the presence of the 30 kDa protein, a more complicated partitioning of actin occurred. At low concentrations of actin, since no spontaneous order of F-actin may occur, only actin bundles were observed in the presence of the 30 kDa protein. At high concentrations of actin (>48 μM where actin alone formed liquid crystals) and 0.5 or 1 μM 30 kDa protein, nematic liquid crystalline domains were observed. However, with increasing concentrations of the 30 kDa protein (2 μM), only actin bundles were observed. Thus, the presence of the 30 kDa protein promoted bundle formation at actin concentrations lower than that required for nematic liquid crystalline domain formation. Moreover, bundle formation was preferred over nematic liquid crystal formation in solutions containing actin at concentrations and lengths suitable for liquid crystal formation if sufficient concentrations of the 30 kDa protein were present.

Light Scattering. Previous results showed that isotropic solutions containing actin alone had values for the ratio of the Hv/Vv scattered light intensity of approximately 0.025. The values of the ratio of the Hv/Vv scattered light intensities increased to 0.3−0.6 with increasing actin concentration which indicated formation of a nematic liquid crystalline phase in the absence of any cross-linking protein (Furukawa et al., 1993). All filament lengths except 0.6 μm (222:1 actin:gelsolin) formed nematic liquid crystalline phases (Figure 3A−C, 0 μM 30 kDa protein).

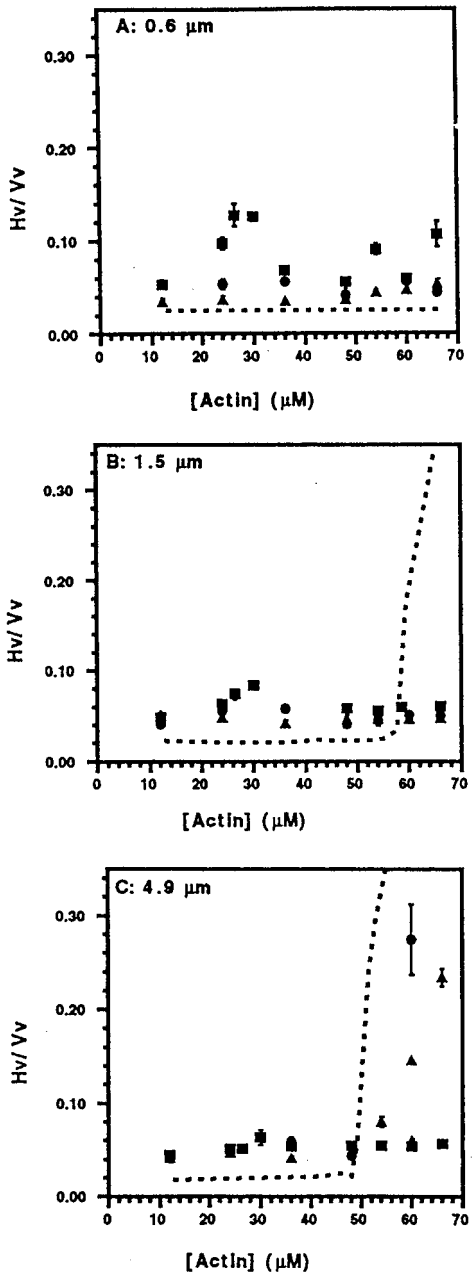

FIGURE 3: Ratio of the Hv/Vv scattered light intensities as a function of actin filament length and the 30 kDa protein concentration. Solutions containing (A) 222:1 actin:gelsolin (0.6 μm), (B) 555:1 actin:gelsolin (1.5 μm), and (C) 1778:1 actin:gelsolin (4.9 μm) and either 0 (- - -), 0.5 μM (▲), 1 μM (●), or 2 μM (■) 30 kDa protein. The mean value and standard deviation are calculated from at least 3 points. Data points for which the error bars are not visible in the figure have standard deviations that are not larger than the symbol. An increasing concentration of the 30 kDa protein causes preferential formation of bundles versus nematic liquid crystals (B and C), while only bundles were formed at 0.6 μm. The formation of bundles was dependent on filament length.

Polarization microscopy allows visual discrimination between actin bundles and liquid crystalline domains but is not quantitative. Light scattering yields quantitative data but cannot discriminate between actin bundles and nematic liquid crystalline domains. Thus, samples were examined using both methods in order to characterize the extent and types of structures which formed.

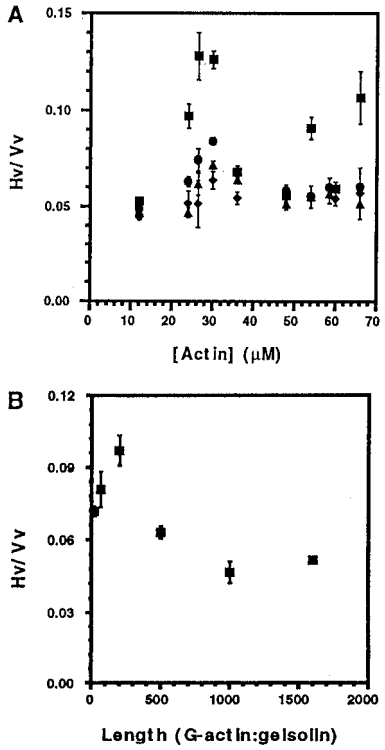

FIGURE 4: Effect of average filament length on formation of actin bundles. A. Solutions containing 2 μM 30 kDa protein and 222:1 actin:gelsolin (0.6 μm) (■), 555:1 actin:gelsolin (1.5 μm) (●), 1111:1 actin:gelsolin (3.0 μm) (▲), or 1778:1 actin:gelsolin (4.9 μm) (◆). The magnitude of the ratio of the Hv/Vv scattered light intensities increases as actin filament length decreases. (B) The concentrations of actin and 30 kDa protein were maintained at 24 and 2 μM, respectively. The actin:gelsolin ratio was varied as indicated. The values of the ratio Hv/Vv of scattered light intensities were measured 24 h after mixing. Orientation is optimal at intermediate filament lengths. Note that bundle formation was observed at all lengths.

The short filaments (0.6 μm in length, 222:1 actin:gelsolin) show an increasing ratio of the Hv/Vv scattered light intensity values over that for actin alone as the concentration of the 30 kDa protein is increased from 0.5 to 1.0 to 2.0 μM at a wide range of actin concentrations (Figure 3A). Long filaments 4.9 μm in length (1778:1 actin:gelsolin) in the presence of 0.5 or 1 μM 30 kDa protein had a large value for the ratio of the Hv/Vv scattered light intensity, indicating the presence of a nematic liquid crystalline phase formation (Figure 3C). As the concentration of the 30 kDa protein is increased to 2 μM in the presence of the same concentration and length distribution of actin, the ratio of the Hv/Vv scattered light intensity decreases, apparently indicating a less ordered solution (Figure 3C). At intermediate filament lengths, the ratio of the Hv/Vv scattered light intensity decreases, apparently indicating a less ordered solution (Figure 3B). These results show that light scattering gives quantitative results consistent with polarization microscopy observations (see above). Also, the light scattering results show that increasing concentrations of the 30 kDa protein at a constant actin concentration and length are more effective in promoting bundle formation.

Bundle Formation as a Function of Filament Length. The effect of filament length on actin bundle formation was studied in the presence of 2 μM 30 kDa protein over a wide range of actin concentrations (Figure 4A). The magnitude of the ratio of the Hv/Vv scattered light intensities reflects

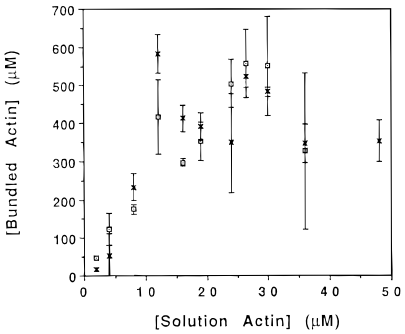

FIGURE 5: Concentration of actin in the bundled portion as a function of the concentration of actin, average actin filament length, and 2 μM 30 kDa protein. The actin concentration in the bundled portion increases to a plateau value of 360−600 μM which is much greater than the concentration of actin in the solution regardless of actin length. Actin:gelsolin ratios were 222:1 (×) and 1778:1 (□). The mean value and the standard deviation are calculated from at least three points. Data points for which the error bars are not visible in the figure have standard deviations that are not larger than the symbol.

bundle formation. The formation of bundles in the presence of the 30 kDa protein is more pronounced for the shortest actin filaments studied.

This effect of actin length on bundle formation was further investigated at a constant actin concentration of 24 and 2 μM 30 kDa protein as a function of the actin:gelsolin ratio. The ratio of Hv/Vv scattered light intensities was a maximum at an actin:gelsolin ratio of 222:1 and decreases as the actin:gelsolin ratio was varied to higher or lower values as shown in Figure 4B. Actin bundling mediated by the 30 kDa protein is more effective with shorter filament lengths. Moreover, a solution containing an actin:gelsolin ratio as low as 22:1 can form bundles as detected by transmission of light through crossed polarizers and light scattering. Thus, in contrast to nematic liquid crystal formation in the absence of a cross-linking protein, actin bundling mediated by the 30 kDa protein is more effective with shorter filament lengths.

Analysis of the Actin Bundle Formation by Low-Speed Sedimentation. Mixtures of actin and the 30 kDa protein in microcapillary tubes were centrifuged at low sedimentation rates to separate the bundled portion from the supernatant. The concentrations of actin and the 30 kDa protein in both the bundled portion and the supernatant and the volume fraction of the bundled portion were measured as described in Materials and Methods.

The concentration of actin in the bundled portion increased as the concentration of the 30 kDa protein was increased from 0.5 to 1 to 2 μM at all actin lengths and concentrations studied. The concentration of actin in the bundled portion increases fairly linearly with solution actin between 2 and 12 μM and was fairly constant at 360−600 μM above solution actin concentrations of 12 μM (2 μM 30 kDa protein, Figure 5) or decreased slightly at the higher actin concentrations (0.5 and 1 μM 30 kDa protein, not shown). This behavior was observed for actin filament lengths of 0.6 and 4.9 μm. The final actin concentrations in the bundled portion are remarkably high, considering that there is at most 48 μM actin in the bulk solution. The concentration of actin in the bundled portion is 20-fold greater than that in the bulk solution at low total actin concentrations and decreases to 10-fold greater as total actin concentration increases to 48 μM. Thus, the presence of the 30 kDa protein concentrated the actin through cross-linking into microdomains.

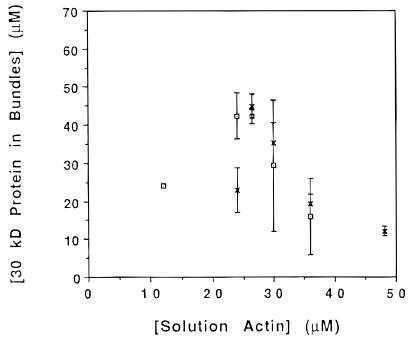

FIGURE 6: Concentration of the 30 kDa protein in the bundled portion as a function of the total actin concentration in the solution and actin filament length in the presence of 2 μM 30 kDa protein in the solution. The concentration of the 30 kDa protein in the bundled portion decreases as the total actin concentration increases. Actin:gelsolin ratios were 222:1 (×) and 1778:1 (□). The mean value and standard deviation are calculated from at least three points. Data points for which the error bars are not visible in the figure have standard deviations that are not larger than the symbol.

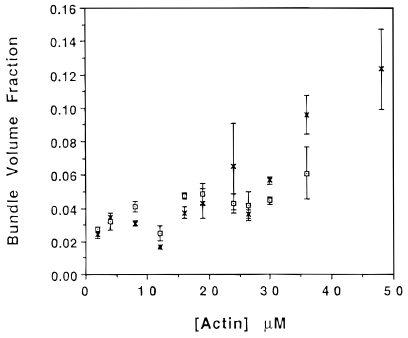

FIGURE 7: Volume fraction of the bundled portion as a function of total actin in solution and average actin filament length in the presence of 2 μM 30 kDa protein. The volume fraction of the bundled portion increases linearly as the concentration of actin in the solution increases. Actin:gelsolin ratios were 222:1 (×) and 1778:1 (□). The mean value and standard deviation are calculated from at least three points. Data points for which the error bars are not visible in the figure have standard deviations that are not larger than the symbol.

The concentration of the 30 kDa protein in the bundled portion was determined as a function of total actin concentration and length in the presence of 2 μM 30 kDa protein as shown in Figure 6 (0.5 and 1 μM 30 kDa protein, not shown). As the concentration of actin in solution increases, the concentration of the 30 kDa protein in the bundled portion decreased from 40 to 10 μM and is not markedly length dependent. The concentration of the 30 kDa protein in the bundled portion is 20-fold greater than that in the bulk solution at low total actin concentrations and decreases to 5-fold greater as the total actin concentration increases to 48 μM. Thus, microdomains contain an actin and 30 kDa protein concentration that is significantly greater than that of the bulk solution.

The stoichiometry of actin and the 30 kDa protein in the bundled portion was calculated for the solutions containing 2 μM 30 kDa protein in the bulk solution. At low concentrations of total actin, there is approximately one 30 kDa protein per actin monomer in the bundled portion. As the concentration of total solution actin increases, the stoichiometry of actin to the 30 kDa protein in the bundled portion increases to 18:1 over the range of actin concentrations investigated. The stoichiometry of actin:30 kDa protein obtained at the highest actin solution concentrations increases as the concentration of 30 kDa protein in the solution decreases from 2 to 1 to 0.5 μM.

The volume fraction of the bundled portion (volume of the bundled portion/total volume) increases as a linear function of the concentration of actin in solution at average actin filament lengths of 0.6 μm (222:1 actin:gelsolin) and 4.9 μm (1778:1 actin:gelsolin) (other lengths not shown) in the presence of 2 μM 30 kDa protein as shown in Figure 7. Lower concentrations of the 30 kDa protein increased the values of the volume fraction to a greater extent, but the volume fraction was still a linear function of the solution actin concentration (0.5 and 1 μM not shown). The magnitude of the volume fraction depends on the concentration of total actin in solution but did not depend on filament length. Bundles formed at actin concentrations as low as 2 μM.

Modeling. Computational modeling of bundling actin filaments by an actin bundling protein reveals an increase in the mean length and the length polydispersity of the filament population as shown in Figure 8A−D. The model also predicts a reduction in the number of filaments as large bundles form at elevated ratios of bundling protein to actin filaments (Figure 8A−D). The mole fraction of the total actin that resides in the bundles was calculated from the computer modeling results as shown in Figure 9. These results were filament length dependent. At a given ratio of bundling protein to actin filaments, longer filaments formed

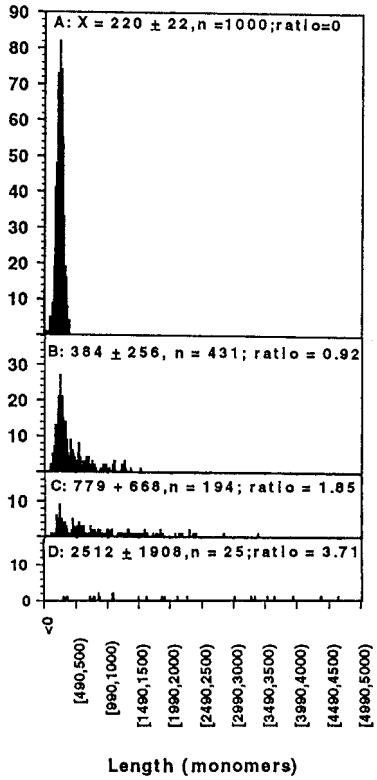

FIGURE 8: Filament/aggregate length distribution predicted by computer modeling depends on the ratio of actin cross-linking protein to actin filaments. The original population had a mean length of 222 monomers, a standard deviation of 22, and an initial population (n) of 1000 filaments (A). As the ratio of actin cross-linking protein to actin filaments increases, the filament length distribution increases toward greater values and the number of cross-linked aggregates decreases (B−D). The average filament length, the standard deviation, the number of filaments remaining in the solution, and the molar ratio of the bundling protein to actin filaments are shown in the figure.

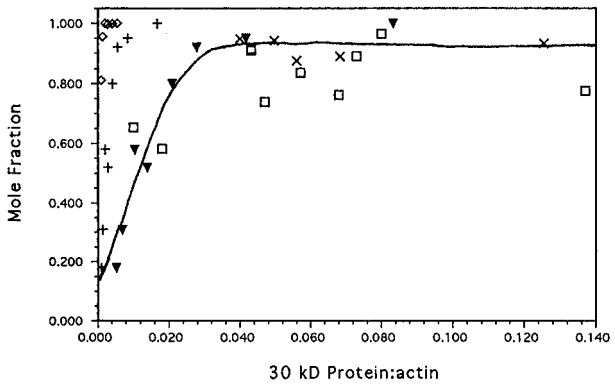

FIGURE 9: Comparison of the mole fraction of the actin in bundles predicted by computer modeling and obtained from the sedimentation assay. Actin:gelsolin ratios were 222:1 (experimental, □; predicted, +; and 5 × predicted, ▼) and 1778:1 (experimental, ×; and predicted, ◇). The line is drawn through 5 × the values predicted for an actin:gelsolin ratio of 222:1.

relatively longer bundled structures and a larger fraction of the total actin resided in bundled structures. Regardless of filament length, the fraction of actin in bundled structures is predicted to increase to near maximum values at relatively low ratios of bundling protein to actin. Further increases in the ratio of bundling protein to actin increase the length of the bundles (Figure 8A−D).

Comparison of the fraction of actin filaments in the bundled portion obtained from computer modeling and from the sedimentation assay is shown in Figure 9. The experimental data confirm the modeling prediction that the mole fraction of actin filaments in the bundled portion, which is defined as any cross-linked filaments, is an increasing function of the ratio of the bundling protein to actin filament concentrations. However, the mole fraction of filaments in the bundled portion increases at lower ratios of bundling protein to actin than is predicted by the experimental data. The agreement between the calculated mole fraction of actin in bundles and experimentally obtained values is within a factor of 5 as shown in Figure 9. Thus, computer modeling appears to reproduce some basic aspects of the mechanism of bundling actin filaments.

DISCUSSION

The formation of isotropic gels or anisotropic bundles of actin filaments cross-linked by actin binding proteins is an exceedingly complex process whose outcome may be influenced by a variety of kinetic and thermodynamic parameters. We have investigated the role of the 30 kDa actin bundling protein in the formation of actin bundles as a function of actin concentration, actin filament length, and 30 kDa protein concentration employing a variety of techniques: transmission of light through crossed polarizers, polarized light microscopy, light scattering, sedimentation, and computer modeling. It is important to use a combination of techniques since any single technique alone could not provide the information obtained using a multifaceted approach.

Actin Length. Formation of actin bundles in mixtures of actin and the 30 kDa protein was observed over a wide range of actin filament lengths. Bundling of actin filaments is quite distinct from spontaneous ordering to form nematic liquid crystals, since at concentrations and lengths of actin filaments not sufficient to promote spontaneous alignment actin can be efficiently bundled by the 30 kDa protein. Moreover, the order achieved in the bundled portion depends markedly on the filament length (Figure 4A,B). Maximum bundle order is achieved with filaments 0.6 μm long (222:1 actin:gelsolin). Filaments longer and shorter than 0.6 μm do not achieve as high a degree of order, although they are bundled. Support for our finding that bundling of very long actin filament populations (~5 μm) is less than optimal comes from the report that bundling of actin by α-actinin is promoted by severing the actin filaments (Maciver et al., 1991). Computer modeling predicts that longer filaments form longer bundles than short filaments at a constant actin bundling protein ratio. The contrast to experimental results is consistent with a role for molecular rearrangement and diffusion in the bundling process (Wachsstock et al., 1993), since shorter filaments may diffuse and rearrange more easily than long filaments to form more ordered bundles.

Actin Concentration. Formation of actin bundles in mixtures of actin and the 30 kDa protein was observed at all concentrations of actin tested between 2 and 65 μM. The concentration of actin in the bundled portion increases fairly linearly with solution actin between 2 and 12 μM and was fairly constant at 360−600 μM above solution actin concentrations of 12 μM (Figure 5). These values are minimal estimates, since the actin concentration in the bundled fraction is an average of that in the bundles and the space between the packed bundles. The concentration of actin in individual actin filament bundles has been estimated to be approximately 3600 μM (Matsudaira et al., 1983). Increases in the solution concentration of actin were linearly related to the volume fraction occupied by the bundled portion (Figure 7). Thus, once the actin concentration was sufficiently high to allow formation of a bundled portion, additional actin resulted in growth of this portion. These results are consistent with data that suggest that bundling depends on the concentration and stoichiometry of actin and actin cross-linking proteins (Stokes & DeRosier, 1991).

Effect of Cross-Linking Protein Concentration on Bundling. The 30 kDa protein promotes bundling of short actin filaments (<1 μm) that are not spontaneously ordered in nematic liquid crystalline domains at the actin concentrations employed. Increases in the concentration of the 30 kDa protein from 0.5 to 2 μM enhanced the formation of bundles at a range of actin concentrations and filament lengths as observed by polarization microscopy and light scattering (Figure 3). The effect of the 30 kDa protein to promote the formation of actin bundles preferentially is apparent in studies of graded increases in the concentration of the 30 kDa protein. Increases in the concentration of the 30 kDa protein promoted bundling for the longest filaments examined (Figure 3C), although actin concentrations were high enough for nematic liquid crystal formation. The concentration of the 30 kDa protein in the bundled portion was 5−20 times greater than that in the bulk solution over a range of concentrations of actin (Figure 6), indicating that both actin and the 30 kDa protein are concentrated in the microdomains.

Computer modeling predicts that longer and fewer bundles will form as increasing amounts of a bundling protein bind to a constant number of actin filaments. The mean length of the bundled filaments is much greater than the initial value, and the distribution of filament lengths is broader and skewed toward longer filament lengths (Figure 8A−D). These

factors will contribute a driving force for actin alignment within the microdomains (see below).

Spontaneous Alignment of Actin Filaments. The spontaneous ordering of actin in the absence of an actin cross-linking protein is an entropy-driven process which depends on the concentration, length, and shape anisotropy of the filaments. When the solution becomes crowded (i.e. more concentrated), spontaneous alignment occurs, reducing the entropy of the particles in the ordered phase while increasing the entropy of the system as a whole. The alignment between the filaments in the nematic phase is high. The fundamental parameter derived from theoretical treatments of phase transitions from rodlike molecules (Onsager, 1949), wormlike chains (DuPre & Yang, 1991), and charged wormlike chains (Sato & Teramoto, 1991) is the volume fraction. For actin, the volume fraction predicted by the Onsager calculation for nematic phase formation is 0.066 when the filaments are 0.6 μm and decreases as the length increases (Furukawa et al., 1993). This volume fraction corresponds to a concentration of actin filaments in the bulk solution of 864 μM. Experimentally, the volume fraction of actin required for the formation of a nematic liquid crystal is significantly smaller than that theoretically predicted and was slightly length dependent (Furukawa et al., 1993). This result was attributed to the length polydispersity of the filaments. When a polydisperse length distribution is present, the longest filaments preferentially enter the nematic phase at a lower volume fraction (lower actin concentration) than a monodisperse length population with the same average length (Odijk, 1986; Lekkerkerker et al., 1984).

This effect of polydispersity can be illustrated by calculating the concentration of actin required for a phase transition for three solutions: (1) monodisperse filaments with length L_1, (2) a mixture of two filaments with lengths L_2 and L_1 with a mole fraction of 0.3 for the species with L_2 and a length ratio L_2:$L_1 = 2$, and (3) solution 2 except that L_2:$L_1 = 5$. In all three cases, L_1 is 0.6 μm (222:1 actin:gelsolin), and the actin filament is modeled as a rigid cylinder with a diameter of 10 nm. The volume fraction for the isotropic to nematic liquid crystalline phase is calculated by the theory of Onsager (1949) or by the theory of Lekkerkerker et al. (1984) for monodisperse or mixtures of uncharged rodlike particles, respectively. For solution 1, the critical concentration required for a phase transition to an ordered state is 864 μM. For the solutions with L_2:$L_1 = 2$ and 5, the concentration decreases to 319 and 77 μM, respectively. Thus, the addition of a small quantity of a longer filament dramatically decreased the concentration of actin required for a phase transition.

Spontaneous Alignment Contributes to Bundling Mediated by the 30 kDa Protein. We propose that spontaneous ordering plays an integral role in the order attained by actin in bundle formation mediated by the 30 kDa protein. The presence of the 30 kDa protein in actin filament solutions causes formation of actin bundles at actin concentrations and filament lengths at which spontaneous alignment is not expected to occur (Figure 2). Cross-linking of the filaments into bundles results in the formation of microdomains that contain high concentrations of actin. The resultant mixture of bundles and filaments forms a population of highly polydisperse length structures. These two conditions allow spontaneous alignment of actin filaments to be a possible mechanism for ordering actin in bundles. This model is supported by polarized light microscopy, light scattering, sedimentation, and computer modeling described herein. First, the minimum estimate of the concentration of actin in the bundled phase was 360−600 μM, approximately 10 times higher (or more, if the effects of polydispersity are taken into effect) than is required for spontaneous alignment (Figure 5). Thus, concentrating the actin in the microdomains could facilitate spontaneous alignment of actin within the bundle. The alignment of actin within the bundles is consistent with the observations of birefringence. Second, the 30 kDa protein is also concentrated in the microdomains which results in a varying actin:30 kDa protein ratio. Third, the computer simulations indicated that the average length and length polydispersity of the population are predicted to increase as the bundling protein:actin filament ratio increases (Figure 8A−D). Length polydispersity lowers the concentration of actin required for a phase transition to the nematic state. This could provide another driving force for actin alignment in bundles. In this way, the increase in actin concentration, length, and length polydispersity caused by the actin bundling protein as formation of microdomains is initiated will provide the driving forces for actin alignment within the bundles.

The role of spontaneous alignment is not inconsistent with earlier mechanistic descriptions of the bundling process. Initial cross-linking events resulting in formation of small microdomains and an increasing volume fraction are consistent with a nucleation and growth model for bundle formation proposed previously (Stokes & DeRosier, 1991). The increased concentration, length, and length polydispersity of the actin in these domains provide a driving force for actin alignment. Redistribution of the filaments through diffusion in these aggregates results in formation of well-ordered arrays. The effects of filament length are consistent with the model that the capacity for rearrangement of initially formed aggregates through diffusion and reversible interactions plays an important role in actin bundle formation (Wachsstock et al., 1993). Note, however, that the polarity of the actin filaments in many types of actin bundles found in vivo and in reconstituted mixtures of actin with actin cross-linking proteins cannot result from spontaneous alignment and must be inherent in the structural interaction of the cross-linking protein with the actin filament.

A final aspect of our data, and of our model, is that short filaments at dilute actin concentrations are observed and expected to be efficiently bundled by this mechanism. This is significant, since most of the filaments in cortical cytoplasm are short, with lengths well below 0.5 μm. In *Dictyostelium*, for example, 97% of the actin filaments are estimated to be about 76 subunits or 0.2 μm (Podolski & Steck, 1990). Filaments as short as 22 subunits at an actin concentration of 24 μM were bundled in the presence of 2 μM 30 kDa protein. In reconstituted mixtures of *Dictyostelium* plasma membranes with actin and the 30 kDa protein, actin promotes binding of the 30 kDa protein and recruitment of additional actin to the membrane (Fechheimer et al., 1994). Rapid assembly of bundled actin could be important in the formation of the filopodia, phagocytic cup, cleavage furrow, and cell to cell contact sites, structures in which actin and the 30 kDa protein have been colocalized (Furukawa & Fechheimer, 1994; Fechheimer et al., 1994; Fechheimer, 1987). Comparative studies of the dynamic properties and mechanisms of actin bundle formation in vitro in the presence

of distinct classes of actin cross-linking proteins will aid in elucidating their contributions to formation of polarized actin structures in cells.

ACKNOWLEDGMENT

The authors thank Dr. Hope T. M. Ritter for the generous use of the polarized light microscope.

REFERENCES

Buxbaum, R. E., Dennerll, T., Weiss, S., & Heidemann, S. R. (1987) *Science 235*, 1511−1514.
Condeelis, J. (1993) *Annu. Rev. Cell Biol. 9*, 411−444.
Cooper, J. A., Bryan, J., Schwab, B., Frieden, C., & Loftus, D. J. (1987) *J. Cell Biol. 104*, 491−501.
Coppin, C. M., & Leavis, P. C. (1992) *Biophys. J. 63*, 794−807.
Cortese, J. D., & Frieden, C. (1988) *J. Cell Biol. 107*, 1477−1487.
Cortese, J. D., & Frieden, C. (1990) *Cell Motil. Cytoskel. 17*, 236−249.
Coue′, M., & Korn, E. D. (1985) *J. Biol. Chem. 260*, 15033−15041.
Detmers, P., Weber, A., Elzinga, M., & Stephens, R. E. (1981) *J. Biol. Chem. 256*, 99−105.
Donald, A. M., & Windle, A. H. (1992) *Liquid Crystalline Polymers*, Press Syndicate of the University of Cambridge, New York.
DuPre, D. B., & Yang, S. (1991) *J. Chem. Phys. 94*, 7466−7477.
Elson, E. L. (1988) *Annu. Rev. Biophys. Biophys. Chem. 17*, 397−430.
Fechheimer, M. (1987) *J. Cell Biol. 104*, 1539−1551.
Fechheimer, M., & Taylor, D. L. (1984) *J. Biol. Chem. 259*, 4514−4520.
Fechheimer, M., & Furukawa, R. (1991) *Methods. Enzymol. 196*, 84−91.
Fechheimer, M., & Furukawa, R. (1993) *J. Cell Biol. 120*, 1169−1176.
Fechheimer, M., Ingalls, H. M., Furukawa, R., & Luna, E. J. (1994) *J. Cell Sci. 107*, 2393−2401.
Frey-Wyssling, A. (1953) *Submicroscopic Morphology of Protoplasm*, 2nd ed., Elsevier Publishing Co., Amsterdam.
Furukawa, R., & Fechheimer, M. (1990) *Dev. Genet. 11*, 362−368.
Furukawa, R., & Fechheimer, M. (1993) *Mol. Biol. Cell 4*, 152a.
Furukawa, R., & Fechheimer, M. (1994) *Cell Motil. Cytoskeleton 29*, 46−56.
Furukawa, R., Kundra, R., & Fechheimer, M. (1993) *Biochemistry 32*, 12346−12352.
Honerkamp, J. (1994) *Stochastic Dynamic Systems*, VCH Publishers, New York.
Janson, L. W., Kolega, J., & Taylor, D. L. (1991) *J. Cell Biol. 114*, 1005−1015.
Johns, J. A., Brock, A. M., & Pardee, J. D. (1988) *Cell Motil. Cytoskeleton 9*, 205−218.
Kerst, A., Chmielewski, C., Livesay, C., Buxbaum, R. E., & Heidemann, S. R. (1990) *Proc. Natl. Acad. Sci. U.S.A. 87*, 4241−4245.
Kolega, J., Janson, L. W., & Taylor, D. L. (1991) *J. Cell Biol. 114*, 993−1003.
Lekkerkerker, H. N. W., Coulon, P., Van der Haegen, R., & Devlieck, R. (1984) *J. Chem. Phys. 80*, 3427−3433.
Luby-Phelps, K., Lanni, F., & Taylor, D. L. (1988) *Annu. Rev. Biophys. Biophys. Chem. 17*, 369−396.
Maciver, S. K., Wachsstock, D. H., Schwarz, W. H., & Pollard, T. D. (1991) *J. Cell Biol. 115*, 1621−1628.
MacLean-Fletcher, S. D., & Pollard, T. D. (1980) *Biochem. Biophys. Res. Commun. 96*, 18−27.
Matsudaira, P. (1991) *TIBS 16*, 87−92.
Matsudaira, P., Mandelkow, E., Renner, W., Hesterberg, L. K., & Weber, K. (1983) *Nature 301*, 209−214.
Meyer, R. K., & Aebi, U. (1990) *J. Cell Biol. 110*, 2013−2024.
Nunnally, M. H., D'Angelo, J. M., & Craig, S. W. (1980) *J. Cell Biol. 87*, 219−226.
Odijk, T. (1986) *Macromolecules 19*, 2313−2329.
Onsager, L. (1949) *Ann. N.Y. Acad. Sci. 51*, 627−659.
Otto, J. J. (1994) *Curr. Opin. Cell Biol. 6*, 105−109.
Podolski, J. L., & Steck, T. L. (1990) *J. Biol. Chem. 265*, 1312−1318.
Press, W. H., Flannery, B. P., Teukolsky, S. A., & Vetterling, W. T. (1988) *Numerical Recipes in C. The Art of Scientific Computing*, Cambridge University Press, Cambridge.
Sato, T., & Teramoto, A. (1991) *Physica A 94*, 72−86.
Seifritz, W. (1942) *The Structure of Protoplasm*, The Iowa State College Press, Ames, IA.
Smith, P. K., Krohn, R. I., Hermanson, G. T., Mallia, A. K., Gartner, F. H., Provenzano, M. D., Fujimoto, E. K., Goeke, N. M., Olson, B. J., & Klenk, D. C. (1985) *Anal. Biochem. 150*, 76−85.
Spudich, J. A., & Watt, S. (1971) *J. Biol. Chem. 246*, 4866−4871.
Stokes, D. L., & DeRosier, D. J. (1991) *Biophys. J. 59*, 456−465.
Suzuki, A., Maeda, T., & Tadanao, I. (1991) *Biophys. J. 59*, 25−30.
Taylor, D. L., & Condeelis, J. S. (1979) *Int. Rev. Cytol. 56*, 57−144.
Taylor, D. L., & Fechheimer, M. (1982) *Philos. Trans. R. Soc. London, Ser. B 299*, 185−197.
Wachsstock, D. H., Schwatz, W. H., & Pollard, T. D. (1993) *Biophys. J. 65*, 205−214.
Wachsstock, D. H., Schwarz, W. H., & Pollard, T. D. (1994) *Biophys. J. 66*, 801−809.
Yin, H. L., Zaner, K. S., & Stossel, T. P. (1980) *J. Biol. Chem. 255*, 9494−9500.

BI9601924